

Multiple Myeloma Regression Mediated by Bruceantin

Muriel Cuendet,¹ Konstantin Christov,²
Daniel D. Lantvit,¹ Yunfan Deng,³
Samad Hedayat,³ Lawrence Helson,⁴
James D. McChesney,⁴ and John M. Pezzuto⁵

¹Program for Collaborative Research in the Pharmaceutical Sciences, Department of Medicinal Chemistry and Pharmacognosy,

²Department of Surgical Oncology, College of Medicine, and

³Department of Mathematics, College of Liberal Arts and Sciences, University of Illinois at Chicago, Chicago, Illinois; ⁴NaPro BioTherapeutics Inc., Boulder, Colorado; and ⁵Purdue University, Schools of Pharmacy, Nursing, and Health Sciences, West Lafayette, Indiana

ABSTRACT

Purpose: Bruceantin has been shown to induce cell differentiation in a number of leukemia and lymphoma cell lines. It also down-regulated c-MYC, suggesting a correlation of down-regulation with induction of cell differentiation or cell death. In the present study, we focused on multiple myeloma, using the RPMI 8226 cell line as a model.

Experimental Design: The effects of bruceantin on c-MYC levels and apoptosis were examined by immunoblotting, 4',6-diamidino-2-phenylindole staining, evaluation of caspase-like activity, and 3,3'-dihexyloxycarbocyanine iodide staining. The potential of bruceantin to inhibit primary tumor growth was assessed with RPMI 8226 xenografts in SCID mice, and apoptosis in the tumors was evaluated by the terminal deoxynucleotidyl transferase-mediated nick end labeling assay.

Results: c-MYC was strongly down-regulated in cultured RPMI 8226 cells by treatment with bruceantin for 24 h. With U266 and H929 cells, bruceantin did not regulate c-MYC in this manner. Apoptosis was induced in the three cell lines. In RPMI 8226 cells, apoptosis occurred through proteolytic processing of procaspases and degradation of poly(ADP-ribose) polymerase. The mitochondrial pathway was also involved. Because RPMI 8226 cells were the most sensitive, they were used in a xenograft model. Bruceantin treatment (2.5–5 mg/kg) resulted in a significant regression of tumors without overt toxicity. Apoptosis was significantly elevated in tumors derived from animals treated with bruceantin (37%) as compared with the control tumors (14%).

Conclusions: Bruceantin interferes with the growth of RPMI 8226 cells in cell culture and xenograft models. These results suggest that bruceantin should be reinvestigated for clinical efficacy against multiple myeloma and other hematological malignancies.

INTRODUCTION

Multiple myeloma is a tumor of the hematopoietic system, accounting for ~12,000 deaths per year in the United States (1). There is a rapid increase in incidence with age and a significant excess at all ages of males. In addition, geographical and racial differences play an important role in the incidence of myeloma. The disease is much more common in African-American populations than in Caucasians, and there is a low incidence in Chinese (1, 2). The roles of genetic background and environment are poorly defined (3).

Multiple myeloma is usually preceded by an age-dependent premalignant disease termed monoclonal gammopathy of undetermined significance. Numeric chromosomal abnormalities are present in virtually all multiple myelomas, and in most, if not all, cases of monoclonal gammopathy of undetermined significance (4, 5). Translocations are common. The incidence of IgH translocations increases with the stage of tumorigenesis (6). Most immunoglobulin translocations involve just three groups of genes: *Cyclins D1–3* (7), *MMSET*, and *FGFR3* (4), and two B-zip transcription factors (c-MAF and MAFB; Ref. 8). Complex translocations dysregulate *c-myc* as a late progression event that is associated with enhanced proliferation. c-MYC is rearranged in 15% of multiple myelomas representing all stages, but this fraction correlates with the severity of disease and is often heterogeneous among cells within the tumor (9). Studies that address the expression of c-MYC RNA and protein in multiple myeloma samples from patients are consistent with increased expression of c-MYC late in the disease (10). Secondary translocations contribute to subsequent progression. Progression from monoclonal gammopathy of undetermined significance to myeloma is associated with activating mutations of *RAS* or *FGFR3*. This progression seems to flip a molecular switch that results in osteolytic bone lesions that are mediated by osteoclastogenesis, neo-angiogenesis and enhanced growth of the myeloma clone (11). Additional tumor progression, and especially extramedullary growth, is associated with increased proliferation, mutations of p53, and secondary translocations that dysregulate c-MYC.

The current therapy for myeloma has relied predominantly on glucocorticoids, such as prednisone, and alkylating agents, primarily melphalan. Neither therapy is curative, and the median survival has remained fixed at ~3 years for the past decade. Although monoclonal gammopathy of undetermined significance can be diagnosed efficiently by a simple blood test, it is not possible to prevent progression or even predict when progression to myeloma will occur. Clearly, there is a need for new drugs that may be useful for the control, treatment, and/or cure of this disease.

Received 3/11/03; revised 10/22/03; accepted 10/22/03.

Grant support: National Cancer Institute Grant P01 CA48112.

The costs of publication of this article were defrayed in part by the payment of page charges. This article must therefore be hereby marked *advertisement* in accordance with 18 U.S.C. Section 1734 solely to indicate this fact.

Requests for reprints: John M. Pezzuto, Purdue University, Schools of Pharmacy, Nursing, and Health Sciences, Heine Pharmacy Building, Room 104, 575 Stadium Mall Drive, West Lafayette, IN 47907-2051.

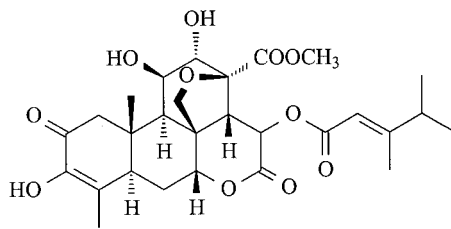


Fig. 1 Chemical structure of bruceantin.

Bruceantin (Fig. 1) is a quassinoid obtained from *Brucea* species (Simaroubaceae). Bruceantin and analogues are capable of inducing an array of biological responses including anti-inflammatory and antileukemic effects with murine models (12). The major mechanism responsible for antineoplastic activity at the molecular level has been attributed to inhibition of protein synthesis (13). Such inhibition has been shown to occur via interference at the peptidyltransferase site, thus preventing peptide bond formation (14). To assess toxicity, bruceantin was evaluated in three separate Phase I clinical trials in patients with various types of solid tumors. Hypotension, nausea, and vomiting were common side effects at higher doses, but hematological toxicity was moderate to insignificant and manifested mainly as thrombocytopenia (15, 16). Bruceantin was then tested in two separate Phase II trials including adult patients with metastatic breast cancer (17) and malignant melanoma (18). No objective tumor regressions were observed, and clinical trials were terminated.

In our program for the procurement of novel plant-derived chemotherapeutic/chemopreventive agents, HL-60 cell differentiation activity has been used as one marker of activity (19). This led to the identification of brusatol (a structural analogue of bruceantin) as a potent inducer of HL-60 cell differentiation (20), and bruceantin was found to demonstrate even greater potency. The effect of brusatol was evaluated with a panel of leukemic cells with representative chromosomal translocations and other gene mutations; the compound induced cell death events in some cell lines and terminal differentiation in others. A significant finding was potent down-regulation of c-MYC oncoproteins. Cell lines expressing high levels of c-MYC oncoprotein were most sensitive to brusatol- and bruceantin-mediated effects (21).

In the present study, we focused on multiple myeloma, using RPMI 8226, U266, and H929 cell lines. In RPMI 8226 cells, c-MYC was strongly down-regulated by treatment with bruceantin (10 ng/ml) for 24 h, and cells underwent apoptosis with an IC_{50} value of ~ 7 ng/ml. This involved the caspase and mitochondrial pathways. There was a much lower induction of apoptosis in U266 and H929 cells, and c-MYC levels were not strongly down-regulated as with the RPMI 8226 cells. Because RPMI 8226 cells were the most sensitive, they were used in a xenograft model. SCID mice were inoculated with RPMI 8226 cells and treated with various doses of bruceantin (0–12 mg/kg) once a discernable tumor mass was present. At higher doses, loss of body weight or lethality was observed. At lower doses, however, tumor growth was completely inhibited without overt toxicity.

MATERIALS AND METHODS

Chemicals

Bruceantin was obtained from the National Cancer Institute, and brusatol was isolated from *Brucea javanica* (16). Test compounds were dissolved in DMSO and stored at -20°C . All of the other compounds were purchased from Sigma Chemical Co. (St. Louis, MO).

Cell Culture

RPMI 8226, U266, and H929 cells were obtained from the American Type Culture Collection (Rockville, MD). The cell lines were maintained in suspension culture using RPMI 1640 (Invitrogen, Carlsbad, CA) supplemented with 10% heat-inactivated fetal bovine serum, 100 units of penicillin/ml, and 100 μg of streptomycin/ml at 37°C in a humidified atmosphere of 5% CO_2 in air. The cell line was routinely tested for *Mycoplasma* contamination.

Quantification of Apoptosis

Cells were treated with various concentrations of bruceantin (2.5, 5, 10, 20, or 40 ng/ml) for 24 h, washed with PBS, and fixed with methanol:acetic acid 1:1 for 30 min at room temperature. Cells were then treated with 4,6-diamidino-2-phenylindole (1 $\mu\text{g}/\text{ml}$) for 15 min at room temperature. 4,6-Diamidino-2-phenylindole staining of the nucleus was observed by fluorescence microscopy. At least 100 cells were counted for each sample. A dose-response curve was constructed and the concentration of bruceantin required to induce apoptosis in 50% of the cell population (IC_{50}) was calculated. The same experiment was performed, adding a caspase-1, -3, -4, and -7 inhibitor (Z-VAD; Calbiochem, San Diego, CA) 1 h before treatment with bruceantin.

Immunoblot Analyses

c-MYC. The expression of c-MYC protein was assessed by immunoblots as described previously (22). In brief, cells (10^6) were treated with brusatol (25 ng/ml) or bruceantin (10 ng/ml) and harvested after 4 or 24 h. Whole-cell pellets were lysed with detergent lysis buffer [1 ml/ 10^7 cells, 50 mM Tris-HCl buffer (pH 8.0), 150 mM NaCl, 1 mM DTT, 0.5 mM EDTA, 1% NP40, 0.5% sodium deoxycholate, 0.1% SDS, 100 $\mu\text{g}/\text{ml}$ phenylmethylsulfonyl fluoride, 1 $\mu\text{g}/\text{ml}$ aprotinin, 2 $\mu\text{g}/\text{ml}$ leupeptin, and 100 μM sodium vanadate] to obtain protein lysates, and protein concentrations were quantified using a bicinchoninic acid kit. Because c-MYC is labile, cell lysates were not frozen, but stored at 4°C until all of the lysates were ready for a particular cell line, then a Western blot was performed. Total protein (30 μg) was separated by 10% SDS-PAGE, electroblotted to polyvinylidene difluoride membranes, and blocked overnight with 5% nonfat dry milk. The membrane was incubated with a 2.5 $\mu\text{g}/\text{ml}$ solution of the primary antibody (Oncogene, Cambridge, MA), prepared in 1% blocking solution, for 2 h at room temperature, washed three-times for 15 min with PBS-T (PBS with 0.1%, v/v, and Tween 20), and incubated with a 1:2500 dilution of horseradish peroxidase-conjugated secondary antibody for 30 min at 37°C . Blots were again washed three-times for 10 min each in PBS-T and developed by enhanced chemiluminescence (Amersham, Piscataway, NJ). Mem-

branes were exposed to Kodak Biomax film and the resulting film analyzed using Kodak (Rochester, NY) 1D Image Analysis Software. Membranes were then stripped and reprobed for β -actin (Sigma).

Caspase-3, -8, -9, BID, and Poly(ADP-ribose) Polymerase (PARP). The expression of caspase-3, -8, -9, BID, and PARP protein was assessed by immunoblots. In brief, cells (10^6) were treated with bruceantin (2.5, 5, 10, 20, or 40 ng/ml) and harvested after 24 h. Whole-cell pellets were lysed with detergent lysis buffer [1 ml/ 10^7 cells, 62.5 mM Tris-HCl buffer (pH 6.8), 6 M urea, 10% glycerol, 2% SDS, 0.00125% bromphenol blue and 5% β -mercaptoethanol], then sonicated for 15 s and incubated at 65°C for 15 min to obtain protein lysates, and protein concentrations were quantified using a bicinchoninic acid kit. Total protein (30 μ g) was separated by 7.5–15% SDS-PAGE, electroblotted to polyvinylidene difluoride membranes, and blocked overnight with 5% nonfat dry milk. The membrane was incubated with anticaspase-3 monoclonal antibody (1:100; Santa Cruz Biotechnology, Santa Cruz, CA), anticaspase-8 polyclonal antibody (1:200; Santa Cruz Biotechnology), anticaspase-9 polyclonal antibody (1:200; Santa Cruz Biotechnology), anti-BID polyclonal antibody (1:1000; BD PharMingen, San Diego, CA), or anti-PARP monoclonal antibody (1:100; Oncogene), prepared, washed, and developed as described above for c-MYC.

Analysis of Mitochondrial Membrane Potential

3,3'-Diethyloxycarbocyanine iodide (DiOC_6) is a dye used to measure mitochondrial membrane potential ($\Delta\Psi_m$). In brief, cells (5×10^6) were treated with bruceantin (2.5, 5, 10, 20, or 40 ng/ml) for 6, 12, 18, or 24 h. Fifteen min before collection of cells after drug treatment, 40 nM DiOC_6 was added to the cells. Cells were washed once with PBS before resuspending in 300 μ l PBS containing 40 nM DiOC_6 and 30 μ g/ml propidium iodide. Fluorescence intensities of DiOC_6 were analyzed by flow cytometry with excitation and emission settings of 484 and 500 nm, respectively. Propidium iodide was added to gate out dead cells. Histograms show only propidium iodide-negative cells.

Analysis of Caspase-3/7-like Activity

The Apo-ONE Homogeneous Caspase-3/7 Assay kit (Promega, Madison, WI) was used to measure the activities of caspase-3/7. Cells (1.5×10^4) were treated with bruceantin (10 ng/ml) for 6, 12, 18, or 24 h in a black 96-well plate. At the end of the treatment, lysis buffer and the substrate (Z-DEVD-rhodamine 110) were mixed and added to the cells. Upon sequential cleavage and removal of the DEVD peptides by caspase-3/7 activity and excitation at 499 nm, the rhodamine 110 leaving group becomes intensely fluorescent. The emission maximum is 521 nm. The amount of fluorescent product generated is proportional to the amount of caspase-3/7 cleavage activity present in the sample. The samples were measured in triplicate. Results were expressed as fold of induction relative to the control (DMSO treated cells).

In Vivo Tumor Growth

RPMI 8226 cells (1×10^7) were injected s.c. into the right rear flank of 6- or 13-week-old male and/or female SCID mice

(Frederick Cancer Research Facility, Frederick, MD). Cells were injected in a final volume of 0.1 ml. The area of inoculation was shaved before inoculation. Approximately 10–14 days after inoculation, or when the tumor size was 5 mm, bruceantin (0–12 mg/kg, dissolved in 100% ethanol, sonicated, and diluted to a 5% ethanol solution with saline) was injected i.p. every 3 days. About 40 days after the inoculation of RPMI 8226, treatment with bruceantin was terminated. The vehicle-treated control tumor-bearing group was divided into two groups. Some of these mice continued to receive the vehicle and others were treated with bruceantin (2.5 or 5.0 mg/kg) every 3 days. Animals were weighed twice weekly and observed daily. Tumors were measured twice a week. The volume at the site of the tumor was calculated in mm^3 according to the formula $(D \times d \times 0.2/6) \times \pi$, where D is the longer diameter and d is the shorter diameter.

At the end of the study, the mice were sacrificed by CO_2 asphyxiation. The tumor masses were dissected from the implantation site and the actual tumor size measured. Parts of the tumor masses were appropriately fixed for immunohistochemistry. Care of all of the mice used in these studies was in accordance with institutional guidelines.

Histopathology and Immunohistochemistry

Specimens from the experimental tumors (11 cases from the 13-week-old female SCID mice xenograft study) were fixed in 10% buffered neutral formalin and embedded in paraffin blocks. Necrosis and mitosis were detected at light microscopy on H&E stained sections. The ApopTag *in situ* hybridization detection kit (Intergen, Purchase, NY) was used to identify the apoptotic cells within mouse tumors as described previously (23). Negative controls included the top sections on each slide that were incubated without digoxigenin-dUTP. At least 1000 cells were counted, and the percentage of apoptotic cells was calculated. The slides were counterstained with methyl green for assessment of tumor morphology (23).

Statistical Analysis Used for the *In Vivo* Study

Tumor growth was analyzed using an unbalanced repeated measures model with a serial covariance structure, and body weight change was analyzed using a linear mixed model with random subject intercept effects. SAS/PROC MIXED software (SAS Institute, Cary, NC) was used to perform the analyses. Data were considered statistically significant at $P < 0.05$. All of the statistical tests were two-sided.

RESULTS

Bruceantin Down-Regulates c-MYC in RPMI 8226 Cells. Because c-MYC deregulation is involved in increased apoptosis and proliferation, and was shown to be down-regulated in a previous study involving 10 different leukemia cell lines (21), we analyzed the status of c-MYC in the RPMI 8226 multiple myeloma cell line after a short exposure (4 or 24 h) to brusatol (25 ng/ml) or bruceantin (10 ng/ml). A high level of c-MYC protein was observed in control samples (Fig. 2). Brusatol (data not shown) and bruceantin induced moderate down-regulation at 4 h and complete down-regulation at 24 h. The status of c-MYC was also analyzed in U266 and H929 cell lines. In U266 cells, the level of c-myc was low and did not change

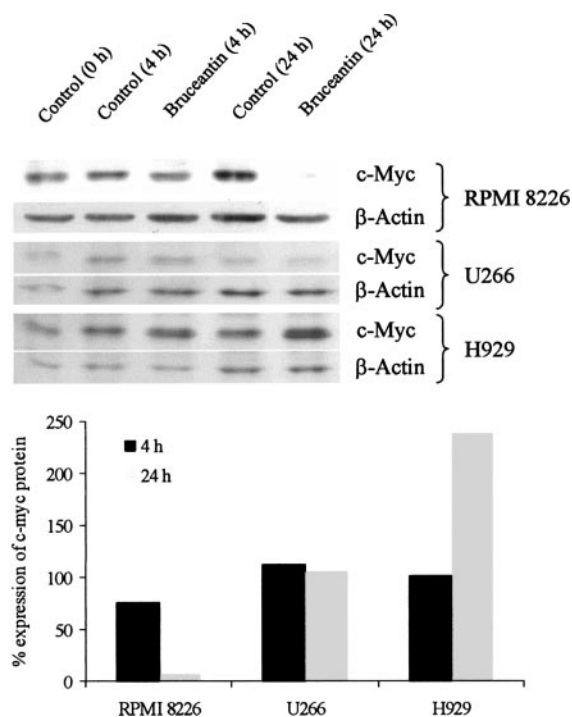


Fig. 2 Bruceantin down-regulates c-MYC expression in RPMI 8226 cells. RPMI 8226, U266, and H929 cells were treated with solvent (0.1% v/v DMSO, control) or bruceantin (10 ng/ml) for 4 or 24 h, and then analyzed by Western blotting. Membranes were probed for c-MYC, and then stripped and probed for β -actin as an internal control. Densitometric analyses results are shown as a percentage of c-myc protein expression relative to levels observed in cells treated with solvent.

after exposure to bruceantin. In H929 cells, bruceantin induced a slight up-regulation at 24 h (Fig. 2).

Bruceantin-Induced Apoptosis Is Dependent on Activation of Caspases. After a 24 h treatment period, concentrations of bruceantin as low as 2.5 ng/ml were shown to induce apoptosis in RPMI 8226 cells, as judged by the formation of apoptotic bodies observed with 4,6-diamidino-2-phenylindole staining. As illustrated by the dose-response curves in Fig. 3, the IC_{50} for apoptosis was 7.0 ng/ml (13 nM) in RPMI 8226 cells, 26.8 ng/ml (49 nM) in U266, and 63.3 ng/ml (115 nM) in H929. To characterize the molecular events associated with bruceantin-induced apoptosis, the effect of a caspase inhibitor (Z-VAD) was investigated. Z-VAD reduced apoptosis to the level of the nontreated cells (Fig. 3). Then we examined whether caspases were activated upon bruceantin treatment. As measured by the fluorometric DEVD-cleavage assay, in RPMI 8226 cells, caspase-3/7-like activity was maximum at 12 h, showing a 3.5-fold induction after cell exposure to bruceantin (10 ng/ml). In U266 and H929 cells, the maximum induction was only ~2-fold after 18 h treatment (Fig. 4). To additionally define the involved caspases, we monitored the processing of caspase-3, -8, and -9, and PARP by Western blots. Treatment of RPMI 8226 cells with bruceantin (2.5, 5, 10, 20, or 40 ng/ml) for 24 h resulted in the proteolytic cleavage of these proteins; the effect was detected at doses of 5 ng/ml and higher (Fig. 5).

Bruceantin Induces Apoptosis through the Mitochondrial Pathway. It has been described that a reduction in $\Delta\Psi_m$ precedes apoptosis and may represent an early signaling event (24). Using the DiOC₆ fluorescent probe, we analyzed the $\Delta\Psi_m$ of RPMI 8226 cells treated with bruceantin. Only 30% of cells showed a $\Delta\Psi_m$ reduction at 6 h with doses between 10 and 40 ng/ml. However, the percentage of depolarized cells reached ~90% when the cells were treated for a longer periods of time (18–24 h; Fig. 6). The involvement of the mitochondrial pathway was also shown by the cleavage of BID (Fig. 5).

Bruceantin Induces Tumor Regression in Xenograft Studies Using SCID Mice. Three independent studies were conducted using 6-week-old female, 13-week-old female, and 6-week-old male SCID mice, measuring the tumor size (Fig. 7). At higher doses, loss of body weight or lethality was observed. Males were more sensitive than females. At lower doses, however, tumors regressed, and their growth was completely inhibited without overt toxicity. In the study using 6-week-old females, a comparison of groups at day 35 showed a tumor volume of 126 mm³ [95% confidence interval (CI), 0–373 mm³] in mice treated with the vehicle or 0 mm³ in mice treated with bruceantin (5, 7.5, or 10 mg/kg). Differences in the growth rate of tumors during the treatment period between the control group and any treated group were statistically significant ($P < 0.0001$). In the study using 13-week-old females, a comparison of groups at day 46 showed a tumor volume of 218 mm³ (95% CI, 0–545 mm³) in mice treated with the vehicle, 26 mm³ (95% CI, 0–57 mm³) in mice treated with bruceantin (1.25 mg/kg), or 0 mm³ in mice treated with 2.5 or 5 mg/kg. Differences in the growth rate of tumors during the treatment period between the control group and any treated group were statistically significant ($P \leq 0.0001$). In the study using 6-week-old males, a comparison of groups at day 35 showed a tumor volume of 274 mm³ (95% CI, 0–763 mm³) in mice treated with the vehicle, or 0 mm³ in mice treated with bruceantin (2.5 or 5 mg/kg). Differences in the growth rate of tumors during the treatment period between the control group and any treated group were statistically significant ($P < 0.0001$ for the groups that received 2.5, 5, or 7.5 mg/kg bruceantin and $P = 0.0003$ for the one that received 10 mg/kg). About 40 days postinoculation, when the control group was divided into two groups, and some of these mice received the vehicle (control group) whereas others received bruceantin (2.5 or 5.0 mg/kg), a statistically significant regression of the tumor was observed in the treated group compared with the control, in all three of the experiments. At day 53, 6-week-old females treated with the vehicle had a tumor volume that increased to 250% (95% CI, 120–383%), compared with 100% at day 35, whereas the tumor volume of mice treated with bruceantin (5 mg/kg) decreased to 5% (95% CI, 0–21%). Differences in the growth rate of tumors during the treatment period between the control and the treated group were statistically significant ($P = 0.0004$). At day 63, 13-week-old females treated with the vehicle had a tumor volume that increased to 176% (95% CI, 0–518%), compared with 100% at day 46, whereas the tumor volume of mice treated with bruceantin (2.5 mg/kg) decreased to 54% (95% CI, 0–177%). Differences in the growth rate of tumors during the treatment period between the control and the treated group were statistically significant ($P = 0.0179$). At day 60, 6-week-old males treated with the vehicle

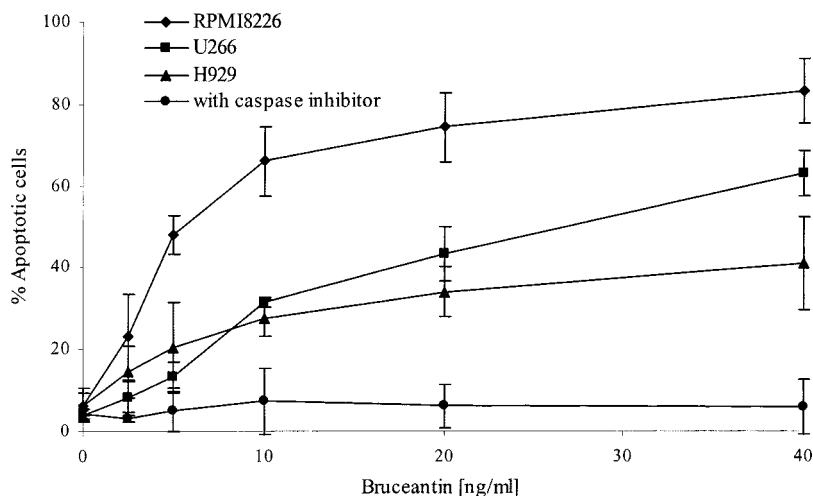


Fig. 3 Dose-dependent induction of apoptosis in RPMI 8226 (◆), U266 (■), or H929 (▲) cells treated with bruceantin (0–40 ng/ml) for 24 h in the absence or presence (●) of caspase inhibitor. Apoptosis was quantified by counting nuclei stained with 4',6-diamidino-2-phenylindole. Results are the means ± 95% confidence interval of three experiments performed in triplicate. Treatments with 2.5 ($P = 0.0361$), 5 ($P = 0.0011$), 10 ($P = 0.0039$), 20 ($P = 0.0016$), and 40 ng/ml ($P = 0.0005$) in RPMI 8226 cells, 10 ($P < 0.0001$), 20 ($P = 0.0025$), and 40 ng/ml ($P = 0.0008$) in U266 cells, and 10 ($P = 0.0067$), 20 ($P = 0.0095$), and 40 ng/ml ($P = 0.0065$) in H929 cells were significantly different from the control values, determined by Student's *t* test.

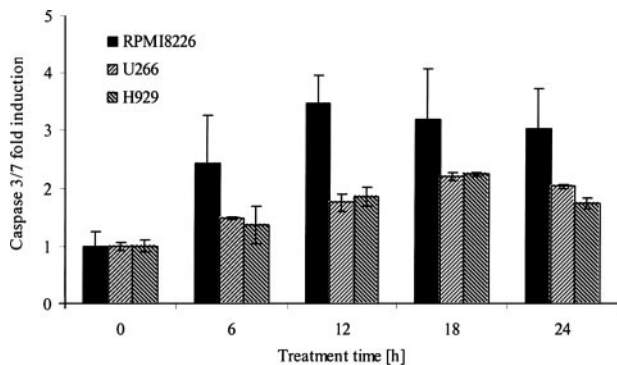


Fig. 4 Caspase-3/7-like activity determined after bruceantin (10 ng/ml) treatment of RPMI 8226, U266, and H929 cells for 6–24 h using the DEVD-R110 cleavage assay. Bars represent the mean ± 95% confidence interval of three experiments. Treatment of RPMI 8226 cells for 6 ($P = 0.0109$), 12 ($P = 0.0066$), 18 ($P = 0.0213$), and 24 h ($P = 0.0170$), of U266 cells for 6 ($P = 0.0014$), 12 ($P = 0.0025$), 18 ($P = 0.0034$), and 24 h ($P = 0.0002$), and of H929 cells for 12 ($P = 0.0388$), 18 ($P = 0.0209$), and 24 h ($P = 0.0434$) were significantly different from the control values, determined by Student's *t* test; bars, ±SD.

had a tumor volume that increased to 318% (95% CI, 0–974%), compared with 100% at day 35, whereas the tumor volume of mice treated with bruceantin (2.5 mg/kg) decreased to 30% (95% CI, 0–130%). Differences in the growth rate of tumors during the treatment period between the control and the treated group were statistically significant ($P < 0.0001$).

Histopathology and Immunohistochemistry. Control tumors were composed of tumor cells forming solid or trabecular structures. The stroma was scanty and the tumor cells were very closely situated (Fig. 8A). Tumor cells in the periphery also infiltrated the surrounding soft tissues. In these areas, tumor cells exhibited high mitotic activity (arrows). The average mitotic index (anaphase + metaphase) per ×40 objective magnification was 12.5% (95% CI, 5–21%). Among the tumor parenchyma, necrotic areas, mostly with central location, were observed frequently.

In the animals treated with bruceantin, the tumor parenchyma was occupied by necrotic areas, which occurred in the peripheral proliferating areas (Fig. 8B), in contrast with the control tumors where the necrosis was in the central areas. Some peripheral tumor areas were replaced by stroma cells, and the tumor architecture was altered as compared with the control tumors. In the areas of tumor tissue disintegration, the frequency of cells with pyknosis and apoptotic nuclei was high (arrows). The number of mitoses in tumors from the treated animals decreased significantly, with an index of 2.2% (95% CI, 1–3%; $P = 0.019$).

The percentage of apoptotic cells evaluated by the terminal deoxynucleotidyl transferase-mediated nick end labeling assay in the peripheral proliferating areas was 14.0% (95% CI,

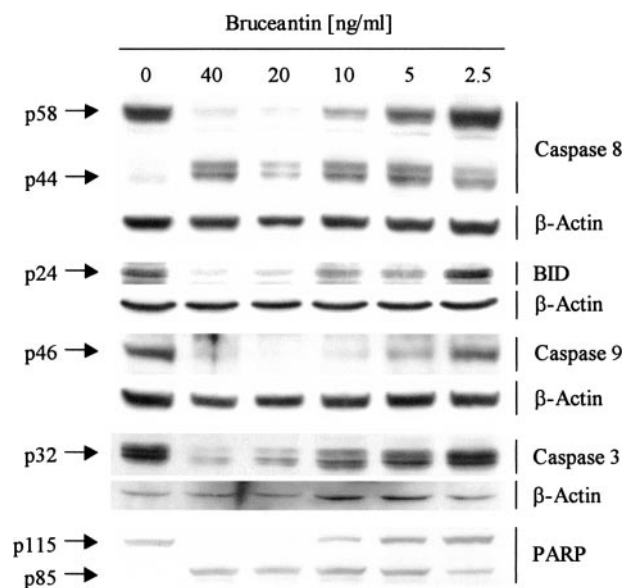
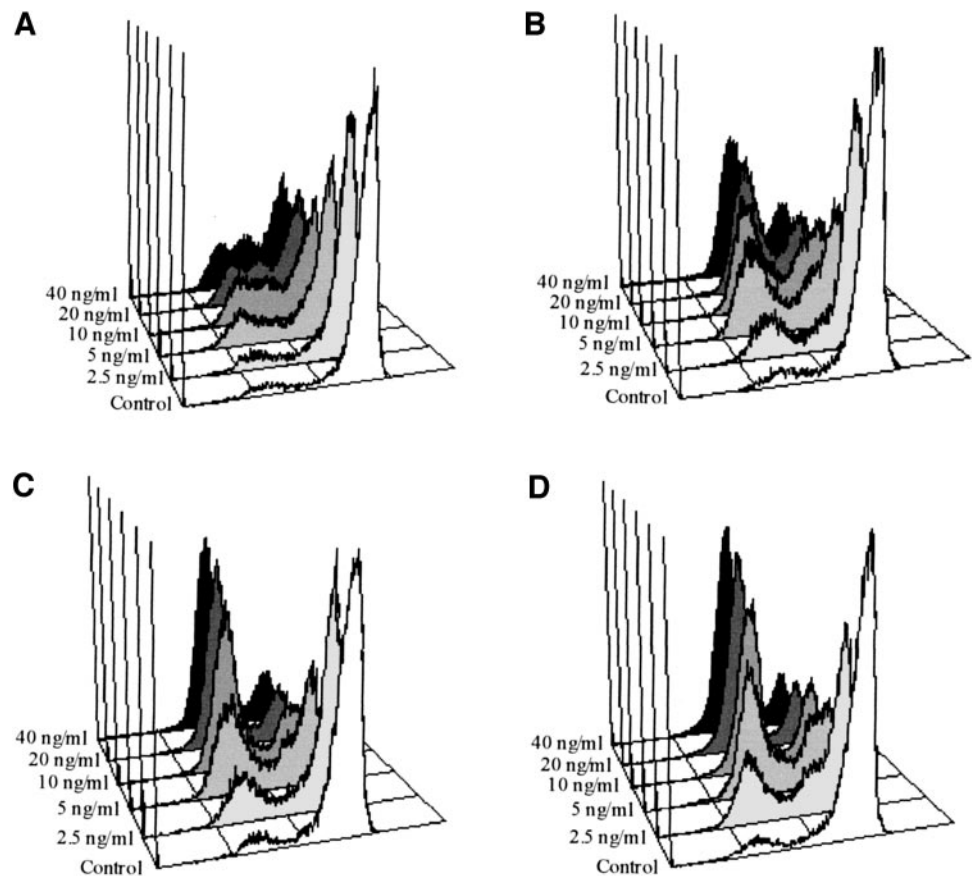


Fig. 5 Dose-dependent cleavage of caspase-8, BID, caspase-9, caspase-3, and poly(ADP-ribose) polymerase (PARP). RPMI 8226 cells were treated with various concentrations of bruceantin (0–40 ng/ml) for 24 h and then analyzed by Western blotting.

Fig. 6 3,3'-Diethyloxycarbonyl iodide labeling of mitochondria. RPMI 8226 cells were treated with the indicated concentrations of bruceantin (0–40 ng/ml) for 6 (A), 12 (B), 18 (C), or 24 h (D), then mitochondrial membrane potential was determined as described in "Materials and Methods."



8–20%) in control tumors (Fig. 8C, arrows), and this significantly increased (36.6%; 95% CI, 15–58%) in the tumors of animals treated with bruceantin (Fig. 8D, arrows, and Fig. 8E; $P = 0.031$). Most apoptotic cells in treated tumors were identified in the peripheral tumor areas.

DISCUSSION

Bruceantin, a quassinoid isolated from *Brucea* species, is known to inhibit protein synthesis (13). We found previously that bruceantin down-regulated c-MYC RNA and protein in 10 different leukemic cell lines, and the extent of activity correlated with this response, based on cell death or terminal differentiation (21). Thus, regulation of c-MYC expression may represent a critical event that leads to cell death or terminal differentiation. In the current study, we used three myeloma cell lines with different *c-myc* gene translocations resulting in deregulation. RPMI 8226 cells have an insertion of a MYC allele in a complex t(16;22) chromosomal translocation (25). In the H929 cell line, complex translocation has interrupted the third exon of the *c-myc* gene (26). As a result of this rearrangement, a chimeric mRNA, much more stable, is expressed. c-MYC is not expressed in the U266 cell line (27). Our results showed that c-MYC expression was down-regulated by bruceantin in RPMI 8226 cells (Fig. 2). In the two other cell lines, U266 and H929, c-MYC expression was not changed or slightly up-regulated by treatment with bruceantin.

Overexpression of c-MYC, or sometimes its down-regulation (28–30), has been shown to induce apoptosis in various cell systems. Thus, apoptosis was analyzed with RPMI 8226, U266, and H929 cells. Treatment with bruceantin resulted in the formation of apoptotic bodies, as observed by 4,6-diamidino-2-phenylindole staining. RPMI 8226 were most sensitive. To elucidate the mechanism underlying proapoptotic effects in further detail, the effect on the activities of various caspases was studied. These cysteine proteases form a proteolytic cascade, which can be initiated by ligation of the cell surface Fas death receptor (31, 32). The present findings that bruceantin led to the proteolytic processing of procaspases-3, -8, and -9, and induced caspase activity, as determined by the DEVD-R110 cleavage assay and the proteolytic degradation of the caspase-3 substrate PARP, indicate that bruceantin-induced apoptosis of RPMI 8226 cells is mediated by this typical death protease cascade. In the three cell lines tested, activation of caspases was necessary for this response, because DNA fragmentation was completely inhibited by the broad-spectrum caspase inhibitor Z-VAD. In RPMI 8226 cells, caspases were activated as early as 6 h after cell exposure to bruceantin, but activation was slower and less intense in U266 and H929 cells. Notably, RPMI 8226 cells were the only cells in which bruceantin induced c-MYC down-regulation, and these cells were the most sensitive to apoptosis. Bruceantin-induced apoptosis was reduced in the two other cell lines where c-MYC was not changed or slightly up-regulated.

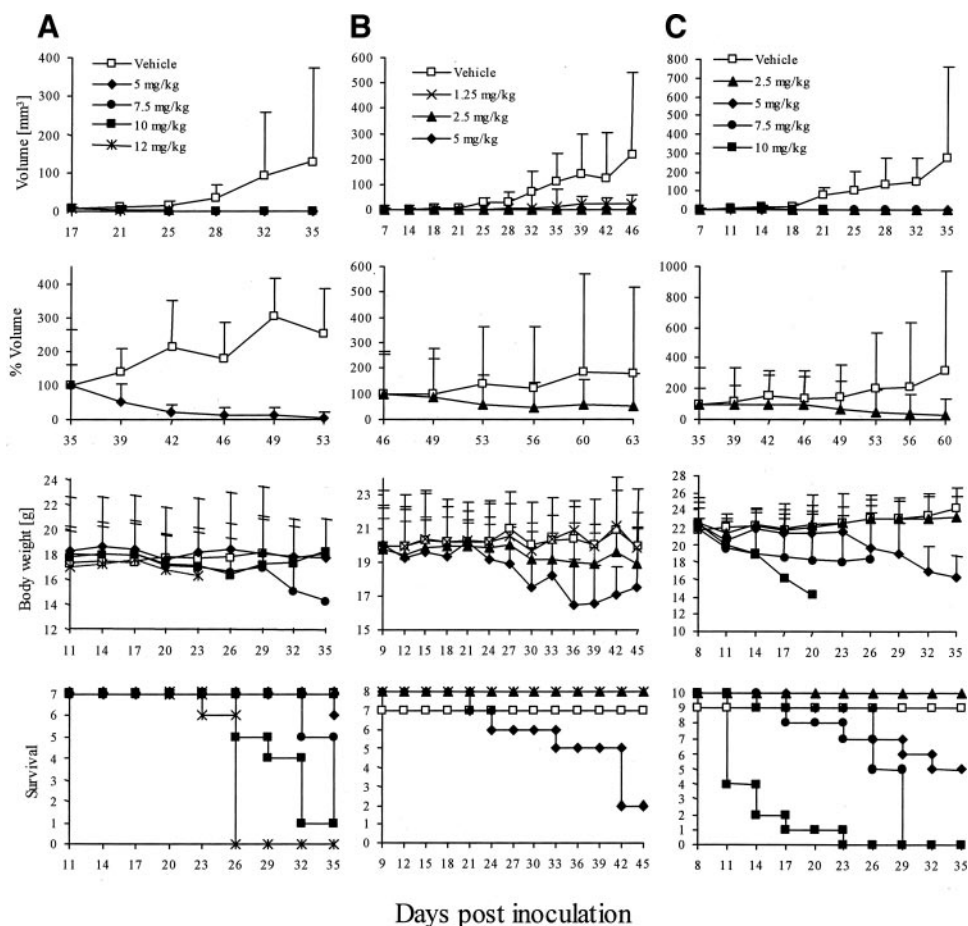


Fig. 7 Effect of bruceantin on the volume of xenograft tumors derived from RPMI 8226 human multiple myeloma cells, mouse body weight, and survival. SCID mice bearing tumors from the transplantation of RPMI 8226 cells were treated with vehicle control (5% ethanol solution in saline) or bruceantin (5–12 mg/kg, every 3 days, i.p.). Tumor diameters were measured, and tumor volumes in mm³ were calculated as described in “Materials and Methods.” Differences in the growth rate of tumors during the treatment period between the control group and the treated groups were statistically significant. **A**, $\sim 1 \times 10^7$ RPMI 8226 cells were inoculated s.c. in the right rear flank of 6-week-old female SCID mice. After day 35, mice from the control group were treated with bruceantin (5 mg/kg, 5 mice) or vehicle (2 mice) until day 53, and the tumor volume was measured. Differences in the growth rate of tumors during the treatment period between the control group and the group treated with 5 mg/kg bruceantin were statistically significant. Body weights were measured twice weekly. There were no statistically significant differences between the control and treated groups. **B**, $\sim 1 \times 10^7$ RPMI 8226 cells were inoculated s.c. in the right rear flank of 13-week-old female SCID mice. After day 46, mice of the control group were treated with bruceantin (2.5 mg/kg, 4 mice) or vehicle (3 mice) until day 63, and the tumor volume was measured. Differences in the growth rate of tumors during the treatment period between the control group and the group treated with 2.5 mg/kg bruceantin were statistically significant. Body weights were measured twice weekly. There was no statistically significant difference between the control and the group treated with 2.5 mg/kg bruceantin, but there was a statistically significant difference between the control group and the group treated with 2.5 and 5 mg/kg bruceantin. **C**, $\sim 1 \times 10^7$ RPMI 8226 cells were inoculated s.c. in the right rear flank of 6-week-old male SCID mice. After day 35, mice of the control group were treated with bruceantin (2.5 mg/kg, 5 mice) or vehicle (4 mice) until day 60, and the tumor size was measured. Differences in the growth rate of tumors during the treatment period between the control group and the group treated with 2.5 mg/kg bruceantin were statistically significant. Body weights were measured twice weekly. There was no statistically significant difference between the control and the group treated with 2.5 mg/kg bruceantin, but there was a statistically significant difference between the control group and the group treated with 5, 7.5, and 10 mg/kg bruceantin. Significantly different from control values when $P < 0.01$. Data are the mean; bars, $\pm 95\%$ CI.

Thus, c-MYC down-regulation induced by bruceantin might be a critical event leading to cell death.

It has been demonstrated recently that the mitochondrial release of cytochrome *c* plays an important role in amplifying the caspase cascade (33, 34). Released cytochrome *c* forms a complex with Apaf-1, resulting in activation of caspase-9 and consequent activation of downstream caspases. Cytochrome *c* release from mitochondria is a consequence of the proteolytic processing of BID (a proapoptotic member of the Bcl-2 family;

Ref. 35), secondary to the activation of caspase-8. Proteolytic generation of the cleaved product of BID results in translocation of BID to the mitochondria and insertion into the mitochondrial membrane where it inhibits the antiapoptotic action of Bcl-2 and results in the release of cytochrome *c*. Western blots showed that bruceantin (5 ng/ml and higher) induced BID cleavage in RPMI 8226 cells. Mitochondrial dysfunction, in particular the induction of the mitochondrial membrane permeability transition, has been implicated in the cascade of events involved in the induc-

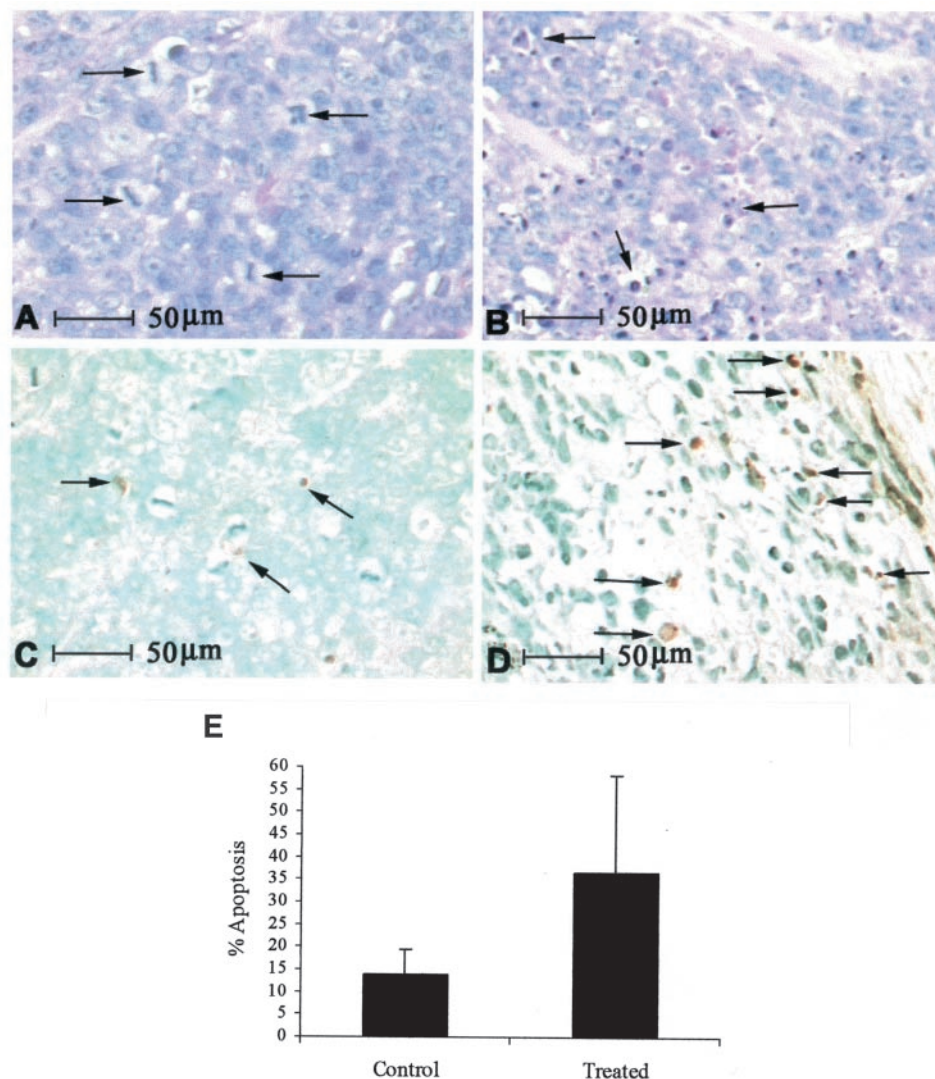


Fig. 8 Effect of bruceantin on mitosis and apoptosis in tumors derived from human multiple myeloma cell line RPMI 8226 in SCID mice. **A**, control tumor with a high number of mitotic figures (*arrows*). Tumor cells are close to each other and there is no necrosis. H&E, $\times 400$. **B**, peripheral tumor area of animal treated every 3 days with bruceantin (2.5 mg/kg) for 17 days. A high number of apoptotic cells (*arrows*) with typical condensation of the chromatin and cytoplasm was observed. Cells with pyknotic nuclei were also frequent in the areas of tumor disintegration. H&E, $\times 400$. **C**, apoptotic cells were identified by the terminal deoxynucleotidyl transferase-mediated nick end labeling assay. There are only a few apoptotic cells (*arrows*) among the parenchyma of control tumors, as well as a high number of mitotic figures. The slide was counterstained with methyl green for identification of tumor morphology, $\times 400$. **D**, tumor of animals treated every 3 days with bruceantin (2.5 mg/kg) for 17 days. Disintegration of tumor parenchyma with a high number of apoptotic cells (*arrows*) as identified by the terminal deoxynucleotidyl transferase-mediated nick end labeling assay. The slide was counterstained with methyl green for identification of tumor morphology, $\times 400$. **E**, percentage of apoptotic cells in tumors derived from RPMI 8226 human multiple myeloma cells in SCID mice treated every 3 days with the vehicle (control) or bruceantin (2.5 mg/kg) for 17 days. More than 1000 cells were counted in each sample. Each data point represents the mean percentage of apoptosis (*bars*, $\pm 95\%$ CI) from four samples. Percentage of apoptotic cells in tumors from treated animals is statistically significantly different from that of control animals, determined by Student's *t* test ($P = 0.031$).

tion of apoptosis. Inhibition of the mitochondrial electron-transport chain reduces the mitochondrial *trans*-membrane potential ($\Delta\Psi_m$), which may induce the formation of the mitochondrial permeability transition pore and the subsequent membrane permeability transition (36). We examined $\Delta\Psi_m$ in bruceantin-treated cells to explore the role of the mitochondria in RPMI 8226 cell apoptosis. Within 6 h of chemical exposure (10–40 ng/ml), a significant percentage of cells exhibited a decreased

incorporation of DiOC₆, indicating the disruption of $\Delta\Psi_m$. This drop in $\Delta\Psi_m$ was both dose- and time-dependent, and correlated well with other parameters of apoptosis. The generation of the cleaved product of BID and the disruption of $\Delta\Psi_m$ in the mitochondria by bruceantin treatment indicates that bruceantin activates the mitochondrial pathway of apoptosis.

RPMI 8226 cells, being the most sensitive to apoptosis, were selected to perform *in vivo* studies. It was found that

bruceantin was effective in treating RPMI 8226 human-SCID xenografts with doses as low as 1.25 mg/kg. Males seemed to be more sensitive to bruceantin than females, but the age of the mice did not affect the response. Doses of 2.5 and 5.0 mg/kg significantly induced regression in early tumors as well as advanced tumors (Fig. 7), without mediating overt toxicity. During the course of this work, we did not attempt to establish optimal dose regimens. However, because human clinical trials have been performed with bruceantin, some rough comparisons can be made. In the mouse, a dose of 2.5 mg/kg body weight injected i.v. theoretically can yield a blood concentration of 75 μM . Obviously, with the dose regimen used in the current study, the average blood concentration must be much lower than this theoretical level. Doses of bruceantin recommended in the Phase I clinical trials were $\sim 5 \text{ mg/m}^2$. In a human of average height and weight, this could theoretically yield a blood concentration of $\sim 3.3 \mu\text{M}$. Clearly, additional preclinical work is required, but it appears that the doses used in our animal studies are sufficiently close to the doses used in the Phase I clinical trials, and it is reasonable to expect that acceptable dose regimens could be devised for human clinical trials. It is encouraging that the concentration required to mediate effects with *in vitro* studies is in the nM range, and significant increases in apoptosis detected by the terminal deoxynucleotidyl transferase-mediated nick end labeling assay with tumor tissue from 13-week-old female SCID mice treated with bruceantin confirmed the relevance of *in vitro* data obtained with RPMI 8226 cells treated with bruceantin.

In summary, with cultured myeloma cells, we demonstrate that apoptotic cell death induced by bruceantin is dependent on c-MYC down-regulation, activation of caspases, and the mitochondrial pathway. With *in vivo* models, at low doses, bruceantin induced complete tumor regression by inhibiting cell proliferation and inducing apoptotic cell death, without mediating overt toxicity. These data suggest that bruceantin should be reinvestigated in a clinical setting for effectiveness against hematological malignancies in which c-MYC is expressed and down-regulated by bruceantin.

ACKNOWLEDGMENTS

We thank the National Cancer Institute for supplying bruceantin and Dr. Karen Hagen of the Research Resources Center (University of Illinois at Chicago) for analysis of samples by flow cytometry.

REFERENCES

- Malpas, J. S., Bergsagel, D. E., Kyle, R., and Anderson, K. Multiple Myeloma: Biology and Management. Oxford: Oxford University Press, 1998.
- Cohen, H. J., Crawford, J., Rao, M. K., Pieper, C. F., and Currie, M. S. Racial differences in the prevalence of monoclonal gammopathy in a community-based sample of the elderly. *Am. J. Med.*, *104*: 439–444, 1998.
- Lynch, H. T., Sanger, W. G., Pirruccello, S., Quinn-Laquer, B., and Weisenburger, D. D. Familial multiple myeloma: a family study and review of the literature. *J. Natl. Cancer Inst.*, *93*: 1479–1483, 2001.
- Drach, J., Schuster, J., Nowotny, H., Angerler, J., Rosenthal, F., Fiegl, M., Rothermundt, C., Gsur, A., Jager, U., and Heinz, R. Multiple myeloma: high incidence of chromosomal aneuploidy as detected by interphase fluorescence *in situ* hybridization. *Cancer Res.*, *55*: 3854–3859, 1995.
- Zandecki, M., Lai, J. L., Genevieve, F., Bernardi, F., Volle-Remy, H., Blanchet, O., Francois, M., Cosson, A., Bauters, F., and Facon, T.

Several cytogenetic subclones may be identified within plasma cells from patients with monoclonal gammopathy of undetermined significance, both at diagnosis and during the indolent course of this condition. *Blood*, *90*: 3682–3690, 1997.

- Bergsagel, P. L., and Kuehl, W. M. Chromosomal translocations in multiple myeloma. *Oncogene*, *20*: 5611–5622, 2001.
- Chesi, M., Bergsagel, P. L., Brents, L. A., Smith, C. M., Gerhard, D. S., and Kuehl, W. M. Dysregulation of cyclin D1 by translocation into an IgH γ switch region in two multiple myeloma cell lines. *Blood*, *88*: 674–681, 1996.
- Chesi, M., Bergsagel, P. L., Shonukan, O. O., Martelli, M. L., Brents, L. A., Chen, T., Schröck, E., Ried, T., and Kuehl, W. M. Frequent dysregulation of the c-maf proto-oncogene at 16q23 by translocation to an Ig locus in multiple myeloma. *Blood*, *91*: 4457–4463, 1998.
- Avet-Loiseau, H., Gerson, F., Magrangeas, F., Minvielle, S., Harousseau, J. L., and Bataille, R. Rearrangements of the c-myc oncogene are present in 15% of primary human multiple myeloma tumors. *Blood*, *98*: 3082–3086, 2001.
- Skopelitou, A., Hadjiyannakis, M., Tsenga, A., Theocharis, S., Alexopoulou, V., Kittas, C., and Agnantis, N. Expression of c-myc p62 oncoprotein in multiple myeloma: an immunohistochemical study of 180 cases. *Anticancer Res.*, *13*: 1091–1095, 1993.
- Bezieau, S., Devilder, M. C., Avet-Loiseau, H., Mellerin, M. P., Puthier, D., Pennarun, E., Rapp, M. J., Harousseau, J. L., Moisan, J. P., and Bataille, R. High incidence of N and K-Ras activating mutations in multiple myeloma and primary plasma cell leukemia at diagnosis. *Hum. Mutat.*, *18*: 212–224, 2001.
- Tang, W., and Eisenbrand, G. *Brucea javanica* (L.) Merr. In: W. Tang, G. Eisenbrand (eds.). Chinese Drugs of Plant Origin: Chemistry, Pharmacology, and Use in Traditional and Modern Medicine, pp. 207–222. Berlin: Springer-Verlag, 1992.
- Liao, L. L., Kupchan, S. M., and Horwitz, S. B. Mode of action of the antitumor compound bruceantin, an inhibitor of protein synthesis. *Mol. Pharmacol.*, *12*: 167–176, 1976.
- Fresno, M., Gonzales, A., Vazquez, D., and Jimenez, A. Bruceantin, a novel inhibitor of peptide bond formation. *Biochem. Biophys. Acta*, *518*: 104–112, 1978.
- Liesmann, J., Belt, R. J., Haas, C. D., and Hoogstraten, B. Phase I study on bruceantin administered on a weekly schedule. *Cancer Treat. Rep.*, *65*: 883–885, 1981.
- Bedikian, A. Y., Valdivieso, M., Bodey, G. P., Murphy, W. K., and Freireich, E. J. Initial clinical studies with bruceantin. *Cancer Treat. Rep.*, *63*: 1843–1847, 1979.
- Wiseman, C. L., Yap, H. Y., Bedikian, A. Y., Bodey, G. P., and Blumenschein, G. R. Phase II trial of bruceantin in metastatic breast carcinoma. *Am. J. Clin. Oncol.*, *5*: 389–391, 1982.
- Arsenau, J. C., Wolter, J. M., Kuperminc, M., and Ruckdeschel, J. C. A phase II study of bruceantin (NSC 165563) in advanced malignant melanoma. *Investig. New Drugs*, *1*: 239–242, 1983.
- Suh, N., Luyengi, L., Fong, H. H. S., Kinghorn, A. D., and Pezzuto, J. M. Discovery of natural product chemopreventive agents utilizing HL-60 cell differentiation as a model. *Anticancer Res.*, *15*: 233–240, 1995.
- Luyengi, L., Suh, N., Fong, H. H. S., Kinghorn, A. D., and Pezzuto, J. M. A lignan and four terpenoids from *Brucea javanica* that induce differentiation with cultured HL-60 promyelocytic leukemia cells. *Phytochemistry*, *43*: 409–412, 1996.
- Mata-Greenwood, E., Cuendet, M., Sher, D., Gustin, D., Stock, W., and Pezzuto, J. M. Brusatol-mediated induction of leukemic cell differentiation and G₁ arrest is associated with down-regulation of c-myc. *Leukemia (London)*, *16*: 2275–2284, 2002.
- Richon, V. M., Webb, Y., Merger, R., Sheppard, T., Jursic, B., Ngo, L., Civoli, F., Breslow, R., Rifkind, R. A., and Marks, P. A. Second generation hybrid polar compounds are potent inducers of transformed cell differentiation. *Proc. Natl. Acad. Sci. USA*, *93*: 5705–5708, 1996.
- Mandlekar, S., Hebbar, V., Christov, K., and Kong, A. N. Pharmacodynamics of tamoxifen and its 4-hydroxy and N-desmethyl metabo-

- lites: activation of caspases and induction of apoptosis in rat mammary tumors and in human breast cancer cell lines. *Cancer Res.*, *60*: 6601–6606, 2000.
24. Zamzami, N., Marchetti, P., Castedo, M., Decaudin, D., Macho, A., Hirsh, T., Susin, S. A., Petit, P. X., Mignotte, B., and Kroemer, G. Sequential reduction of mitochondrial transmembrane potential and generation of reactive oxygen species in early programmed cell death. *J. Exp. Med.*, *182*: 367–377, 1995.
25. Fabris, S., Storlazzi, C. T., Baldini, L., Nobili, L., Lombardi, L., Maiolo, A. T., Rocchi, M., and Neri, A. Heterogeneous pattern of chromosomal breakpoints involving the *MYC* locus in multiple myeloma. *Genes Chromosomes Cancer*, *37*: 261–269, 2003.
26. Hollis, G. F., Gazdar, A. F., Bertness, V., and Kirsch, I. R. Complex translocation disrupts *c-myc* regulation in a human plasma cell myeloma. *Mol. Cell. Biol.*, *8*: 124–129, 1988.
27. Jernberg-Wiklung, H., Pettersson, M., Larsson, L-G., Anton, R., and Nilsson, K. Expression of *myc*-family genes in established human multiple myeloma cell lines: *L-myc* but not *c-myc* gene expression in the U-266 myeloma cell line. *Int. J. Cancer*, *51*: 116–123, 1992.
28. Jamerson, M., Johnson, M., and Dickson, R. Dual regulation of proliferation and apoptosis: *c-myc* in bitransgenic murine mammary tumor models. *Oncogene*, *19*: 1065–1071, 2000.
29. Pelengaris, S., Rudolph, B., and Littlewood, T. Actin of *myc* *in vivo*-proliferation and apoptosis. *Curr. Opin. Genet. Dev.*, *10*: 100–105, 2000.
30. Fuhrmann, G., Rosenberger, G., Grusch, M., Klein, N., Hofnamm, J., and Krupitza, G. The *myc* dualism in growth and death. *Mutat. Res.*, *437*: 205–217, 1999.
31. Nagata, S. Apoptosis by death factor. *Cell*, *88*: 355–365, 1997.
32. Budihardjo, I., Oliver, H., Lutter, M., Luo, X., and Wang, X. Biochemical pathways of caspase activation during apoptosis. *Ann. Rev. Cell Dev. Biol.*, *15*: 269–290, 1999.
33. Yabuki, M., Tsutsui, K., Horton, A., Yoshioka, T., and Utsumi, K. Caspase activation and cytochrome c release during HL-60 cell apoptosis induced by a nitric oxide donor. *Free Radic. Res.*, *32*: 507–514, 2000.
34. Gree, D., and Reed, J. Mitochondria and apoptosis. *Science (Wash. DC)*, *281*: 1309–1312, 1998.
35. Kaufmann, S., and Hengartner, M. Programmed cell death: alive and well in the new millennium. *Trends Cell Biol.*, *11*: 526–534, 2001.
36. Kroemer, G., Petit, P., Zamzami, N., Vayssiere, J-L., and Mignotte, B. The biochemistry of programmed cell death. *FASEB J.*, *9*: 1277–1287, 1995.